Journal of
Applied Crystallography
ISSN 0021-8898

Received 30 October 2008
Accepted 14 January 2009

Online collection and analysis of X-ray fluorescence spectra on the macromolecular crystallography beamlines of the ESRF

Gordon A. Leonard, V. Armando Solé, Antonia Beteva, José Gabadinho,‡ Matias Guijarro, Joanne McCarthy, Dario Marrocchelli,¶ Didier Nurizzo, Seán McSweeney and Christoph Mueller-Dieckmann*

ESRF, BP 220, 38043 Grenoble Cedex 9, France. Correspondence e-mail: muellerd@esrf.fr

X-ray fluorescence (XRF) measurements on solutions or crystals of biological macromolecules provide additional information that can be used in structure determination and/or refinement protocols. Here details are presented of an experimental setup, employed on all the ESRF Macromolecular Crystallography Group beamlines, that allows the online collection and qualitative analysis of XRF spectra. This experimental setup uses a highly attenuated beam and short exposures, meaning it is minimally destructive but retains high sensitivity.

1. Introduction

X-ray fluorescence detectors are standard equipment on synchrotron-based tunable beamlines for macromolecular crystallography (MX) where they are usually used in the scanning of absorption edges of anomalous scatterers contained in crystals. These absorption edges are then analysed in order to choose the wavelength(s) for data collection in multi- or single-wavelength anomalous dispersion (MAD, SAD) experiments designed to solve the phase problem in MX.

X-ray fluorescence (XRF) spectroscopy can also be used, however, to carry out other types of experiments, for example (i) to confirm the presence of a particular anomalous scatterer in a crystal in order to allow a more complete description of crystal contents during structure refinement or (ii) to identify an anomalous scatterer found as a result of the analysis of diffraction data collected earlier. In the latter case, the presence of an anomalous scatterer has generally not been suspected and its presence has not been taken into account when planning the diffraction experiment. Moreover, around 30% of the proteins in a genome contain metal-ion binding sites (Hasnain & Hodgson, 1999; Hasnain, 2004) but they are not always annotated as such.

In both the cases described above, it would, for obvious reasons, be better to identify any anomalous scatterers present in a crystal before data collection takes place. The information obtained concerning the presence of anomalous scatterers can then be used to plan the subsequent experiments and will result in a more efficient use of beam time. While offline techniques such as microPIXE (proton-induced X-ray emission; Garman, 1999) and total reflection X-ray fluorescence spectrometry (TXRF; Mertens *et al.*, 2001) can also be used to provide this information, these procedures are cumbersome and require special sample preparation and equipment. Online, at-beamline collection and analysis of such spectra using standard experimental setups would be a far better proposition. We describe here the hardware and software implemented on the ESRF MX beamlines that allow for the straightforward, rapid (of the order of seconds) and low X-ray dose collection and analysis of XRF spectra from crystals and/or solutions of biological macromolecules.

It should be noted that the collection and analysis of XRF spectra need not be confined to tunable beamlines. Provided the incident X-ray energy is sufficiently high, fluorescence can be induced from almost all elements likely to be present in crystals or solutions of the

‡ Present address: Paul Scherrer Institut, CH 5232 Villigen PSI, Switzerland.
¶ Present address: School of Chemistry, University of Edinburgh, Scotland.

Table 1
X-ray absorption edge and fluorescence emission line energies for elements naturally occurring in macromolecular samples.

All energies have been taken from the *X-ray Data Handbook* (Thompson *et al.*, 2001). Energies that are accessible and can be recorded are in bold. Elements that are automatically detected in an XRF spectrum are given in italics.

	K-shell emission line (keV)		*L*-shell emission line (keV)			
Element	$K_{\alpha1}$	$K_{\beta1}$	$L_{\alpha1}$	$L_{\beta1}$	*K*-edge absorption energy (keV)	L_{III}-edge absorption energy (keV)
Carbon	0.28				0.28	
Nitrogen	0.39				0.41	
Oxygen	0.52				0.54	
Sodium	1.04	1.07			1.07	
Magnesium	1.25	1.30			1.30	
Phosphorus	**2.01**	**2.14**			2.15	0.14
Sulfur	**2.31**	**2.46**			2.47	0.16
Chlorine	**2.62**	**2.82**			2.82	0.2
Potassium	**3.31**	**3.59**			3.61	0.29
Calcium	**3.69**	**4.01**			4.04	0.35
Vanadium	**4.95**	**5.43**	0.51	0.52	5.47	0.51
Chromium	**5.41**	**5.95**	0.57	0.58	**5.99**	0.57
Manganese	**5.90**	**6.49**	0.64	0.65	**6.54**	0.64
Iron	**6.40**	**7.06**	0.71	0.72	**7.11**	0.71
Cobalt	**6.93**	**7.65**	0.78	0.79	**7.71**	0.78
Nickel	**7.48**	**8.26**	0.85	0.87	**8.33**	0.85
Copper	**8.05**	**8.91**	0.93	0.95	**8.98**	0.93
Zinc	**8.64**	**9.57**	1.01	1.03	**9.66**	1.02
Selenium	**11.22**	**12.50**	1.38	1.42	**12.66**	1.43
Bromine	**11.92**	**13.29**	1.48	1.53	**13.47**	1.55
Molybdenum	17.48	19.61	**2.29**	**2.34**	**20.00**	2.52
Iodine	28.61	32.29	**3.94**	**4.22**	33.17	**4.56**

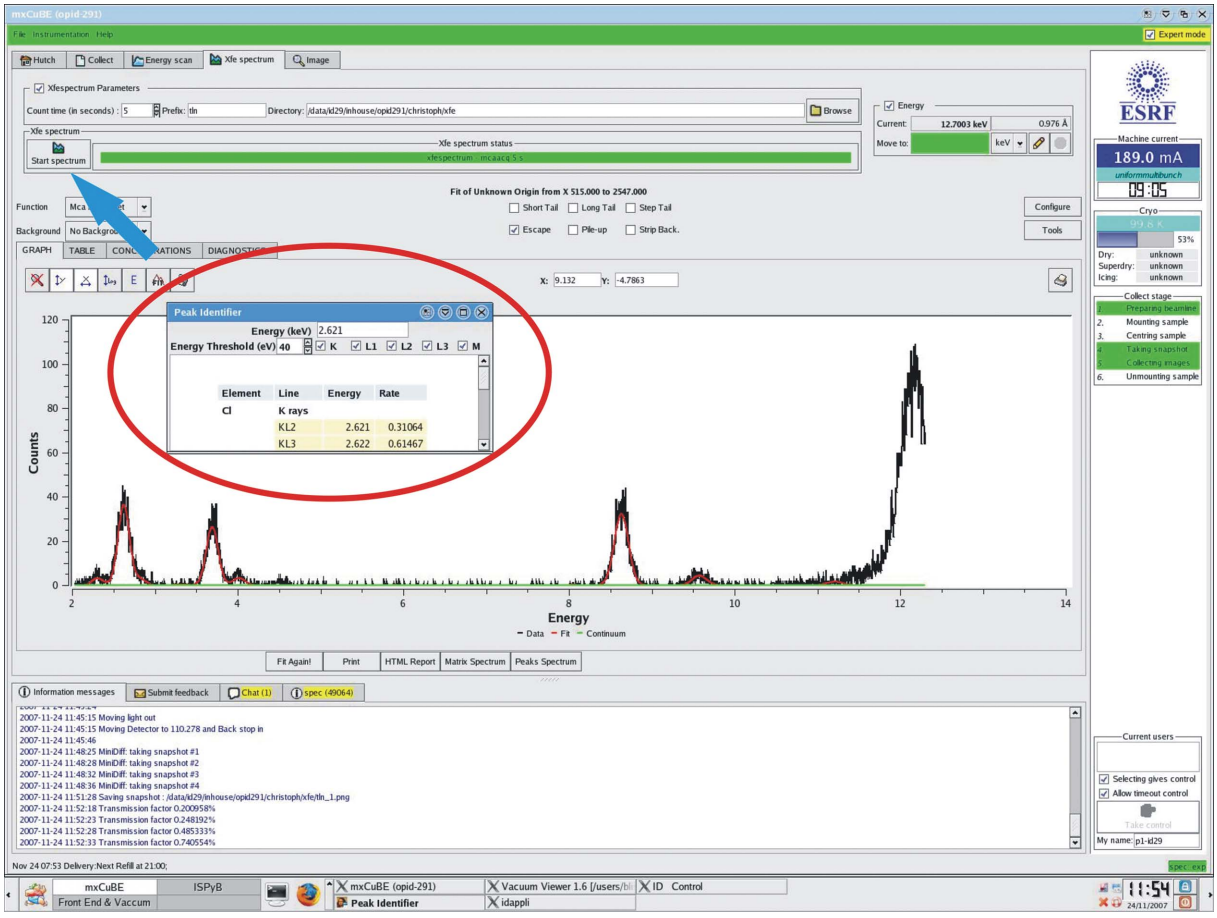

Figure 1
X-ray fluorescence data collection and analysis menu within *mxCuBE*. To record a spectrum, an exposure time needs to be chosen and the *start spectrum* button (highlighted by a cyan arrow) clicked. The software automatically determines the minimum transmission to obtain a sufficient signal on the fluorescence detector. After data collection, a fit is performed to detect elements naturally occurring in proteins. When clicking on a peak in the spectrum, a pop-up window (highlighted with a red ellipsoid) opens, showing all elements with a fluorescence emission line at the chosen energy. The list is sorted by fluorescence yield.

systems usually studied by MX (Table 1). We have thus also implemented the setup described on the fixed-wavelength beamlines of the ESRF MX Group.

2. Description and operation

In the standard experimental setup seen on all the ESRF MX beamlines, silicon drift diode (SDD) detectors coupled with XFlash MMAX signal processing units (XFlash 5010, Bruker AXS Microanalysis, Germany) have been installed. The detector itself is mounted at ∼45° relative to the sample position and X-ray beam, a configuration that allows the detection of X-ray fluorescence from samples mounted on the goniometer rotation axis. The SDDs, which have an active area of 10 mm^2, are mounted on a translation table so that they can be inserted or removed from the sample position as required. To reduce the background noise, a 1.5 mm-diameter detector entrance nozzle has been added. Although the device has a relatively high energy resolution (123 eV at the Mn K_α emission line), this is not sufficient to reveal different redox states of the same metal.

The collection of XRF spectra is extremely straightforward (Fig. 1) and is achieved *via* the *mxCuBE* graphical user interface (GUI; Leonard *et al.*, 2007). The first part of the procedure prior to the collection consists of (i) positioning the fluorescence detector nozzle close to the sample and (ii) defining a minimum transmission of the incident X-ray beam with which a sufficiently large signal is obtained. This is done in order to minimize the exposure of the sample to X-rays and thus to minimize radiation damage to samples that may yet be used for full diffraction data collection. Exposure times are usually in the range of a few seconds. The collected spectrum is analysed using *PyMCA* (Solé *et al.*, 2007) which, based on the energies of the emission lines recorded, checks for the presence of a number of predefined elements (Table 1) and calculates the integrated area under the emission lines.

Control of the data collection and analysis of the XRF spectrum is handled by the *SPEC* software (Certified Scientific Software; http://www.certif.com) underlying *mxCuBE*. I/O signals are read and generated by a modular field bus system from Wago (http://www.wago.com), with *SPEC* controlling the parameters both for the hardware modules and for event timing. *mxCuBE* itself uses a TCP/IP socket to connect to *SPEC* and displays both the spectrum itself and the results of the *PyMCA* element search. It also provides a GUI allowing further, user-directed analysis of the spectrum (Fig. 2).

Fig. 2(*a*) shows an example of an XRF spectrum collected on ESRF MX beamline ID29 from a crystal of thermolysin. The incident beam energy was 12.7 keV and, to collect the spectrum, the crystal was exposed for 5 s using a beam transmission of ∼1% (∼5 × 10^{11} photons). Fig. 2(*b*) shows the results of the *PyMCA* element search. As can be seen, the spectrum contains X-ray emission lines characteristic of Cl, Ca and Zn, and these have been annotated as such.

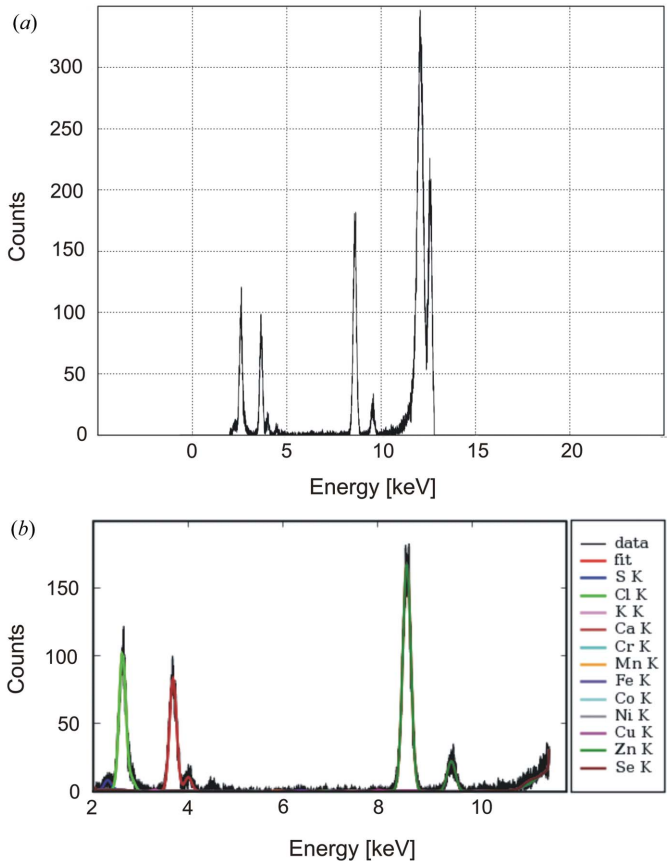

Figure 2
X-ray fluorescence spectrum for thermolysin. (*a*) Raw data showing counts (arbitrary scale) on the detector as a function of energy. The two large peaks at the right in the spectrum are the Compton (inelastic) and the Rayleigh (elastic) scattering peaks. (*b*) The same data as presented in the beamline control GUI *mxCuBE*. In the GUI, for the sake of clarity, only those emission lines ∼1 keV below the energy of the incident beam (in this case 12.7 keV) are shown. The raw data are shown as the black line while the coloured lines are the fit for a series of different, predefined elements (shown in the box to the right of the graph) to the peaks found in the spectrum. From left to right, the fluorescence contains emission lines for S (in blue at 2.3 keV), Cl (in light green at 2.6 keV), Ca (in dark red at 3.7 and 4.0 keV, $K\alpha$ and $K\beta$ fluorescence, respectively) and Zn (in dark green at 8.6 and 9.6 keV, $K\alpha$ and $K\beta$ fluorescence, respectively).

This is consistent with the non-protein atom substructure for thermolysin which consists of eight Cl^- ions, three Ca^{2+} ions and one Zn^{2+} ion (Mueller-Dieckmann *et al.*, 2007).

3. Benefits and limitations

The main benefits of the online, at-beamline XRF spectrum analysis that we describe above are as follows.

(1) It provides experimenters with a rapid, easily accessible and reliable way of elucidating which atoms are present in a crystal and thus provides evidence that can be used to help improve the description of atomic models used in structure refinement.

(2) Metalloproteins typically have a metal-ion binding preference which reflects their physiological function. XRF spectra are ideal tools to show the binding of metal ions to a protein. Thus, a protein that has been reported to bind Fe can be checked rapidly to see if it exclusively binds Fe or also other metals like Zn, Cu or Mn.

(3) It provides experimenters with a rapid, easily accessible and reliable way of assessing whether crystals of a new, uncharacterized protein bind metal ions. Positive evidence that it does, as well as very strong evidence as to the nature of the ion, will suggest MAD/SAD experiments to be performed in order to solve the substructure and, in many cases, will obviate the (time-consuming) need for the incorporation of other anomalous scatterers into the crystal in order to allow structure solution.

(4) XRF spectra can obviate the need to confirm heavy atom derivatization using diffraction data analysis (isomorphous or anomalous difference Patterson maps). After soaking a macromolecular crystal in a solution containing several different heavy atom compounds and after careful back-soaking, XRF analysis can be used to determine if one of these heavy atoms is bound to a protein in a crystal.

(5) The technique can be used to confirm quickly the presence of a substrate/substrate analogue or cofactor, provided they contain a detectable element such as Br or I.

The main limitation of the technique as implemented on the ESRF MX beamlines is that there may be artefacts due to the cryoprotectant that surrounds the crystal. Also, under the current experimental setup, the analysis gives no reliable assessment of how many metal ions a protein might bind. This limitation may be surmountable by using an internal standard of known concentration (*e.g.* 1 m*M* scandium) within the cryoprotectant solution. If more than one type of metal ion is present, calculation of the relative concentrations of these, and thus the ratio of non-protein atoms present, is dealt with automatically within the program *PyMCA*.

4. Conclusion

At the ESRF MX beamlines, we have implemented an online and at-beamline tool to rapidly collect and analyse X-ray fluorescence spectra from macromolecular samples. This allows users to obtain (rapidly) additional information about their samples and, in particular, may prove helpful in diffraction data collection experiment design and/or structure refinement.

A short description of the experiment can also be found at http://www.esrf.eu/UsersAndScience/Experiments/MX/About_our_beamlines/ID29/x-ray-fluorescence-spectrum-xfe-spectrum.

References

Garman, E. (1999). *Structure*, **7**, R291–R299.
Hasnain, S. S. (2004). *J. Synchrotron Rad.* **11**, 7–11.
Hasnain, S. S. & Hodgson, K. O. (1999). *J. Synchrotron Rad.* **6**, 852–864.
Leonard, G. A., McCarthy, J., Nurizzo, D. & Thibault, X. (2007). *Synchrotron Rad. News*, **20**, 18–24.
Mertens, M., Rittmeyer, C. & Kolbesen, B. O. (2001). *Spectrochim. Acta B*, **56**, 2157–2164.
Mueller-Dieckmann, C., Panjikar, S., Schmidt, A., Mueller, S., Kuper, J., Geerlof, A., Wilmanns, M., Singh, R. K., Tucker, P. A. & Weiss, M. S. (2007). *Acta Cryst.* D**63**, 366–380.
Solé, V. A., Papillon, E., Cotte, M., Walter, Ph. & Susini, J. (2007). *Spectrochim. Acta B*, **62**, 63–68.
Thompson, A., Attwood, D., Gullikson, E., Howells, M., Kim, K.-J., Kirz, J., Kortright, J., Lindau, I., Pianetta, P., Robinson, A., Scofield, J., Underwood, J., Vaughan, D., Williams, G. & Winik, H. (2001). *X-ray Data Handbook*, edited by D. Vaughan. Lawrence Berkeley National Laboratory, Berkeley, CA, USA.